Spring 2022

Wetting Transition on 3D-Printed Surfaces

Isabelle Moryan
ijm19@uakron.edu

Analysis of the Wetting Transition on 3D-Printed Featured Surfaces

Isabelle Moryan

Department of Chemical, Biomolecular, and Corrosion

Honors Research Project

Submitted to

The Williams Honors College
The University of Akron

Approved:

Bi-min Zhang Newby Date: 4/20/2022
Honors Project Sponsor (signed)

Bi-min Zhang Newby
Honors Project Sponsor (printed)

R. Gitiafroz Date: 4/20/2022
Reader (signed)

Roya Gitiafroz
Reader (printed)

Edward Evans Date: 4/20/2022
Reader (signed)

Edward Evans
Reader (printed)

Accepted:

Bi-min Zhang Newby Date: 4/20/2022
Honors Department Advisor (signed)

Bi-min Zhang Newby
Honors Department Advisor (printed)

Date: 04/21/2022
Department Chair (signed)

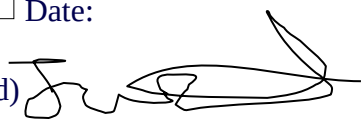

Jie Zheng
Department Chair (printed)

Table of Contents

Executive Summary

This project continued earlier work to further the investigation of manipulating surface features to create superhydrophobic and/or superoleophilic surfaces for organic liquid solutions. Nature naturally produces textured surfaces, such as lotus leaves, to prevent rain from penetrating and "wetting" the surface. This discovery can be used in practical applications such as effectively separating oil/water solutions on plastic surfaces. For this research, deionized (DI) water and oils with different surface tensions were tested on 3-D printed grooved surfaces. The focus was to follow the penetration of a liquid droplet into a grooved surface and determine the optimal surface structures that prevented DI water from penetrating the grooves from the formed contact angles. In addition, the surfaces were tested in favor of allowing oil to spontaneously wet the grooves while the DI water would sit on top of the surface.

The models' cylindrical pillars were 3D-printed in arrays with varying spacing (S) and configurations while maintaining constant pillar diameter (D) and height (H). Two main configurations were studied: hexagonal and square to test how these different configurations could prevent or promote liquids penetration. The model surfaces were also modified, using organosilanes, to obtain different wettability. DI water was the first liquid tested on untreated and treated model surfaces. The droplet size was held at a constant 10 µL for consistency.

The slightly hydrophilic untreated surfaces did not retain DI water droplets on top of the features of various configurations. The square arrangement (spacing 250 µm) had a larger water contact angle at 117±1.6º than the hexagonal array (spacing 250 µm) at 138±13º. Thus, the square arrangement was concluded to be more suitable for creating a super-hydrophobic surface. Increasing the spacing in the hexagonal arrangements from 250 µm to 500 µm showed a decrease in penetration time, from 14 to 3 minutes, and a smaller contact angle for DI water, from 138±13º to 94±4.1º. Meanwhile, the perflouro-organosilane (FTS) treated models became

more hydrophobic, preventing the water and even some oil droplets from penetrating into the grooves of the models. For the spacing 250 μm models, the contact angle became 117±10.9^{o} for the square and >150±0.0^{o} for the hexagonal arrangements. Beyond DI water, n-octane and n-decane solutions were tested on the models. These oils, though, did not have any liquid retention on the untreated surface due to their weak polarity and low surface tension. However, when tested on FTS, the droplets were able to hold their shape for a longer period of time. Weaker carbon chains, n-decane, penetrated quicker than stronger carbon chains, n-octane. A hydrocarbon organosilane, octadecyltrichlorosilane (OTS) was also used to treat the surfaces of the models; however, all the tested oils penetrated quickly into the groove while water droplets retained on top of the features.

The 3D printer used was limited by its resolution and only could print features in hundreds of microns. In future studies, a higher resolution 3D printer should be considered to create smaller pillars in terms of diameter, height, and spacing. Also, the top caps of the features were rounded (i.e., convex), causing water to easily slip into the grooves to wet the surface. Other feature tops should be considered, such as a flat top or even a concave top, for the study.

From this research, I gained skills in professional laboratory work and can effectively work in a high-pressured environment. With this opportunity, I can now use this research to propel myself in the workforce for jobs specializing in polymers. Insights gained from this research can be utilized in technology featuring effective oil/water separation, preventative measures such as bacteria adhesion and metal corrosion and improving human necessities such as blood type compatibility and fog harvesting. Fog harvesting is used to harness water droplets in clouds for consumption. For further research, additional geometric arrays, untested liquids,

and droplet volume should be considered. This research extends a new perspective on the knowledge of droplet behavior on featured surfaces.

Introduction

Nature naturally produces surfaces with hydrophobic characteristics. Lotus leaves, butterfly wings, and even human skins are examples of surfaces designed to repel liquid. These properties are important to developing human necessities. These attributes have been shown to prevent bacteria adhesion, metal corrosion, improve blood type compatibility, lower surface icing in humid atmosphere conditions, and constitutive parts of water storage systems.

This honors project continued the research previously done on printed featured surfaces to confirm the accuracy and expand the examination with new features. These features were modified with hydrocarbon and fluorocarbon organosilanes to observe the changes in surface tension against liquid. In addition, various liquids were examined to determine how quickly each dissipated into the grooves of the texture surfaces. The insight gained from this project can continue the research of human necessities.

An example of a naturally produced hydrophobic surface is the *Colocasia esculenta,* or the Taro leaf. This leaf, on a microscopic scale, shows a honeycomb-like surface that allows water to brush off without wetting the surface. Looking further, the nanoscopic scale showed a flake-like texture that was rough to the touch. In addition, a wax coating on the leaf was noted as an additive to the hydrophobic properties.[1]

When a droplet of water touches the *Colocasia esculenta*, instead of entering the grooves, the droplet remains round with an angle larger than 180^{o} and sits on top. This angle was observed due to the water touching the surface at fewer points and instead of being pulled flat, it is pulled down from the cavities.[2]

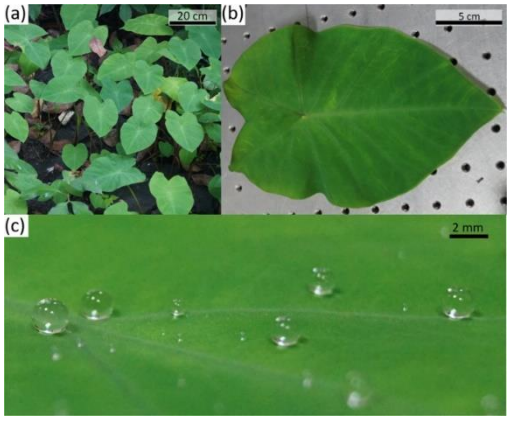

Figure 1 a) *Colocasia esculenta* leaves as they appear in nature.[1] b) A close up of a *Colocasia esculenta* leaf.[1] c) Water droplets on the *Colocasia esculenta*.[1]

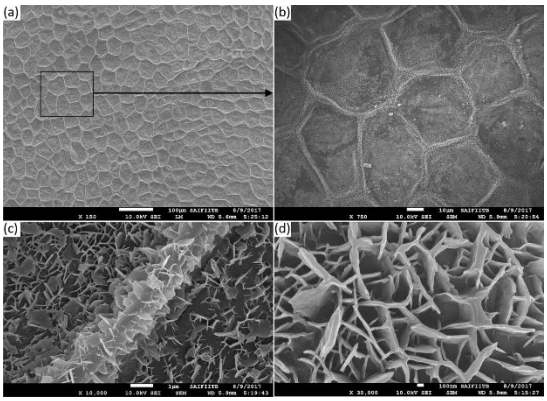

Figure 2 a-d) A microscopic magnification of the *Colocasia esculenta* surface at (a) 50x (b) 750x (c) 10000x and (d) 30000x.[1]

With the inspiration of nature, previous reports have shown effort to engineer non-wettable surfaces through other materials. Researchers from the Indian Institute of Technology Bombay created an epoxy-based polymer to emulate the structure found in the *Colocasia esculenta.* Over 70% of the honeycombs were sized out to be hexagons, rather than pentagons, and became the basis of the surface texture. From their research, increasing the height of the hexagons resulted in an increase in contact angle.[2] Increasing the thickness, however, resulted in a decrease in contact angle. It was also observed the epoxy-based polymer showed the droplet refusing the bounce back off the surface and instead latching onto it. Instead, a small part of the droplet would fall while the remaining would still be on the surface.

This research can be used in future development in water harvesting by capturing condensation. Fog harvesting can help meet water requirements in areas with little rainfall.

Background

Two equations have been developed in literature to explain the alteration of the contact angle over time from an intrinsic contact angle (Θ_s). These include the Wenzel (**Equation 1**) and Cassie-Baxter (**Equation 2**) equation. In the Wenzel equation, Θ_{Wenzel} is the contact angle and r is the surface roughness factor. In the Cassie-Baxter equation, $\Theta_{Cassie\text{-}Baxter}$ is the contact angle, f is the area fraction occupied by the material, and 1-f is the fraction occupied by the air.

$$Cos\theta_{Wenzel} = rcos\theta_s \quad (1)$$

$$Cos\theta_{Cassie-Baxter} = rfos\theta_s - (1-f) \quad (2)$$

These equations apply to the liquid drop sitting on top of the features, trapping the air inside the grooves and assumes the grooves will never be replaced with liquid. To account for the criteria where the liquid penetrates the grooves, it is important to take note of the following relationships. When Θ_s is less than 90^o, the liquid drop enters the Wenzel state as shown in Equation 3.

$$Cos\theta_s \geq \frac{1-f_s}{r-f_s} \quad \text{when } \theta_s < 90^o \quad (3)$$

Where f_s is the ratio of the surface features areas to the total surface from an aerial view. In addition, the Cassie-Baxter state (**Equation 4**), or the contact angle of the flat surface, can be described when Θ_s is greater than 90°.

$$Cos\theta_s \leq -\frac{1-f_s}{r-f_s} \quad \text{when } \theta_s > 90^o \text{ (4)}$$

These relationships can be adjusted by changing the f_s and r, or the ratio of the true surface area of the features to the aerial view total area of the surface. The ratio, f_s, is dependent on spacing (S) and diameter (D) of the features. This ratio is directedly proportional to D and inversely related to S. Meanwhile, the ratio, r, is dependent on the height (H), spacing (S) and diameter (D) of the features. This ratio is directly proportional to D and H and inversely proportional to S. To apply these relationships, r should decrease when Θ_s is less than 90° and increased when Θ_s is greater than 90°. This relationship will create a more hydrophobic surface, a more desirable result.

The contact angle reaches its three-phase contact line when viewed from the side where one can see the drop sitting on the surface. This contact line can be obstructed by the features; thus, it was decided to use a top view of the drop to observe the relationship with the drop radius to the contact angle. This relationship can be described with **Equation 5a and b**.

$$V = \frac{\pi}{3}R^3(2+cos\theta)(1-cos\theta)^2 \quad \text{when } \theta < 90^o \text{ (5a)}$$

$$V = \frac{4\pi}{3}R^3 - \frac{\pi}{3}R^3(2-\cos(180-\theta)+\cos(180-\theta)^3 \quad \text{when } \theta \geq 90^o \text{ (5b)}$$

These equations relate the contact angle to the volume (V) and radius (R) of the droplet. **Equation 5a** applies only when Θ is less than 90° and **Equation 5b** applies only when Θ is greater than 90°. These equations were applied to this project due to the simplicity of determining the volume and radius. Only droplet volumes of ≤ 10 μL were used from a measured capillary (This number is less than the critical capillary number).

Experimental Methods

Pre-created polymer surfaces were designed in a hexagonal and square array from the Stratasys Object260 Connex3 polyjet 3D printer. The printer has a layer resolution of 16 μm and an accuracy of 200 μm. With this technology, the pillar diameter (D) was held constant at 250 μm and pillar height (H) was held constant at 1000 μm. The pillar spacing (S) was varied from 250 to 500 μm to analyze the wettability and impact of a changing spacing ratio (S/D). Three arrangements were tested and evaluated for this project.

The first objective of this project was to imitate the results from previous research. A droplet of DI water measuring about 10 μL was tested on a square and two hexagonal surfaces with no treatment. This droplet was measured by a VWR 2-20 μL pipette to keep consistency in volume. The droplet was monitored with cameras facing the top and the side of it. Pictures were taken over 5 second intervals in a 30-minute period to ensure the entire wetting process was captured. The time taken to transition from Cassie-Baxter's state (non-wetting state) to the

Wenzel's state (wetting state) was recorded during this interval. From these pictures, the base radius of the droplet was calculated from the cross-sectional area of the droplet. With the volume consistent and the radius determined, the contact angle was able to be determined with **Equation 5**. Each featured surface had three runs to ensure consistency.

The second objective of this project was to expand the research with new treated surfaces and droplets of organic solvents, i.e., oils. For surfaces, the three types of features were air plasma treated for 10 minutes at high power in a Harrick Plasma Cleaner PDC-32G and then modified using a perfluoro organosilane (FTS treated) by submerging the plasma treated model in a 0.5 wt.% FTS in hexane solution for 1 hour. After removing the model from the FTS-hexane solution, it was thoroughly washed with a copious amount of fresh hexane to remove un-grafted FTS from the model surface and dried with a stream of dry air. A similar procedure was followed first with testing DIde-ionized (DI) water droplets on the FTS treated surfaces. Next, the n-ocatane and n-decane droplets were analyzed on the untreated and the FTS treated surfaces to evaluate how the contact angle varied.

For n-octane, it is important to note the untreated surfaces showed no sign of a liquid droplet retention on the features. A video has been included in **Appendix B** to show these results.

Another treatment of the surface was considered. This treatment was with octadecyl trichlorosilane (OTS) and followed the same procedure as treating with FTS but using a 0.5 wt.% OTS solution in hexane instead. DIDI water, n-octane and n-decane were used at a constant 10 μL to test treated models. To increase visibility of the liquid, the liquid was dyed with a food dye.

A separate experiment using a mixture of water/n-octane was carried out to roughly assess the oil/water separation efficiency of the untreated, FTS and OTS treated models. The droplet of mixture was dyed with food colorings, blue for water and red/orange for n-octane, to increase visibility on the behaviors of the oil/water mixture. These videos and some selected images on the oil/water separation are included in **Appendix B.**

Data and Results

The parameters for the featured surfaces with cylindrical pillars calculations were done to predict if the droplet would transition from the Cassie-Baxter state to the Wenzel state. When these quantities are compared to the cosine values of the contact angle like in **Equation 5**, the expectation of the model can be predicted. It was determined that both the untreated and FTS state of the examined surfaces were predicted to remain in the Cassie-Baxter state for DI water.

Table 1 The three featured surfaces examined with their respective diameter (D), radius (R), spacing (S), and ratio (S+D) in micrometers (µm). With these values, the expected r and fs values were able to be determined for a consistent pillar height (H) of 1000 µm for this project.

						H (µm):	1000
Feature	**D (µm)**	**R (µm)**	**S (µm)**	**S+D (µm)**	**fs**	**r**	**(1-fs)/(r-fs)**
Square	250	125	250	500	0.196	4.14	0.204
Hexagon	250	125	250	500	0.226	4.63	0.176
Hexagon	250	125	500	750	0.101	2.61	0.358

Table 2 The measured apparent contact angles (Θ_s**)** of DI water for the square featured surfaces. In addition, the cosine of the contact angle was included to help evaluate the predicted state of the model. It was determined that both the untreated and FTS surfaces would stay in the Cassie-Braxter state.

Surface	**Θ_s**	**Cos Θ_s**
Untreated	94.62	-0.080
FTS	117.83	-0.467

The untreated and FTS models both showed the same prediction due to the impact of the grooves. Previous research showed that the resin used in the models' creation was somewhat polar and would be more hydrophilic. This relationship is shown since the contact angle was smaller for the untreated surface compared to the FTS surface, however, the features both predicted the model to remain in the Cassie-Braxter state.

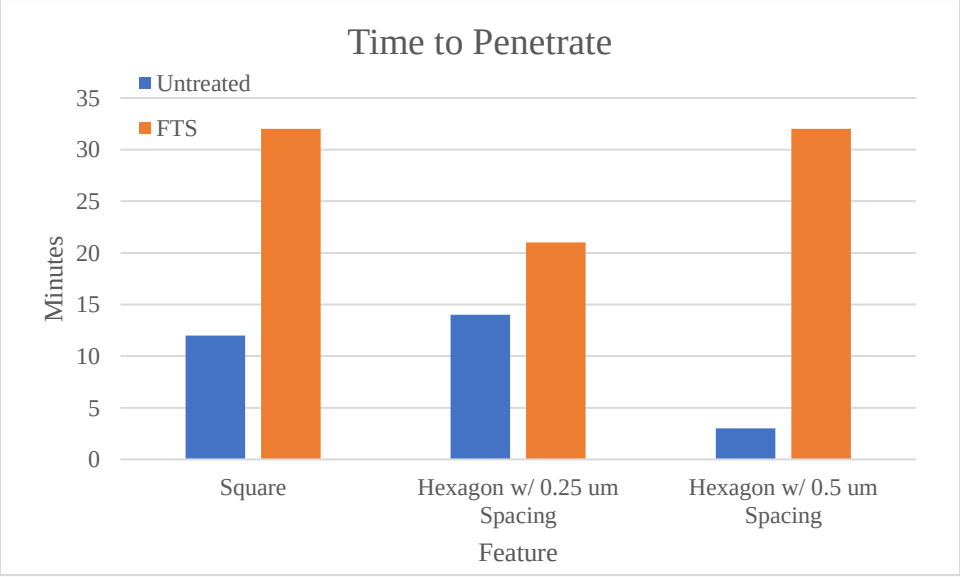

Figure 3 The estimated time to penetrate or evaporate for DI water for the three main features observed. For the untreated surfaces, it was shown that the hexagonal arrangement (of the same spacing) was more hydrophobic than the square arrangement. However, when the spacing was increased from 250 µm to 500 µm, the penetration time decreased significantly. For the FTS

surface, it is clear to see this produced a very hydrophobic surface compared to the untreated surface. The same trends, also, held true.

For DI water, the untreated surfaces remained much closer to the Wenzel angle estimation from **Equations 1 and 2**. However, when treated with FTS, these angles became much larger and aligned more closely with the Cassie-Baxter angle estimation. This result shows the FTS treated surface is much more hydrophobic than the untreated surface. It is also important to note the square feature had a consistent contact angle for both the untreated and FTS surfaces due to the arrangement.

For the square models, the droplet showed signs of penetration early on, sooner than the hexagonal model with the same spacing (250 μm), making this arrangement less desirable. When treated with the air plasma treatment (FTS), the surface became extremely hydrophobic and much more desirable by maintaining the Cassie-Baxter state for a long period of time (From **Figure 3**). This observation is depicted in **Figure 4**.

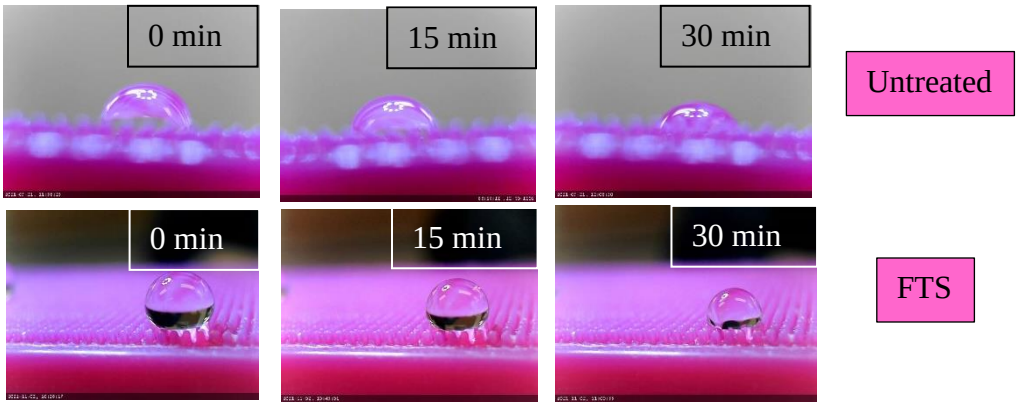

Figure 4 The time scale from when a 10 μL water droplet was initially placed on the surface of a square feature. The droplet enters the Wenzel state on the untreated surface while remains in the Cassie-Baxter state for the FTS surface. Evaporation, in addition, was also more noticeable for the droplet on the FTS treated surface.

For the hexagonal models, changing the spacing from 250 to 500 μm led to a decrease in average contact angle as expected. The time for penetration, also, decreased as spacing increased. When treated with FTS, this trend remained true, however, the angles were much larger, which aligned closer to the Cassie-Baxter criteria.

Table 3 Shows the untreated surface angles for DI water. The feature arrangement, diameter (D), height (H), and spacing (S) are all listed accordingly below. The average angle over the entire tested period (30 minutes) was calculated and shown along with the standard deviation. In addition, the predicted angles from **Equations 1 and 2** for the Wenzel and Cassie-Baxter estimations are shown above.

Surface	**Untreated**							
Solution	**DI Water**							
Feature	**D (μm)**	**H (μm)**	**S (μm)**	**Average Angle (º)**	**St.dev (º)**	**Average R (μm)**	**Wenzel Estimation (º)**	**C-B Estimation (º)**
Square 1	250	1000	250	117	1.6	1.37	128.84	153.30
Square 2	250	1000	250	108	2.8	1.44	116.93	149.94
Hexagon	250	1000	500	94	4.1	1.56	97.22	155.14
Hexagon	250	1000	250	138	13	1.27	161.34	160.39

Table 4 Shows the FTS surface angles for DI water. The feature arrangement, diameter (D), height (H), and spacing (S) are all listed accordingly below. The average angle over the entire tested period (30 minutes) was calculated and shown along with the standard deviation. In addition, the predicted angles from **Equations 1 and 2** for the Wenzel and Cassie-Baxter estimations are shown above.

Surface	**FTS**							
Solution	**DI Water**							
Feature	**D (μm)**	**H (μm)**	**S (μm)**	**Average Angle (º)**	**St.dev (º)**	**Average R (μm)**	**Wenzel Estimation (º)**	**C-B Estimation (º)**
Square	250	1000	250	117	10.9	1.34	128.70	153.55
Hexagon	250	1000	500	114	7.4	1.39	125.60	160.28
Hexagon	250	1000	250	>150	0.0	1.01	150.69	165.84

Beyond varying the spacing, two other solutions (n-octane and n-decane) were tested. For the untreated surfaces, the organic solutions failed to have the droplet retain in either Wenzel or Cassie-Baxter state and immediately penetrated the features. This is due to their chemical chains having weaker polarity than water. Pictures and a video showing this relationship for n-octane can be found in **Figure 5** and **Appendix B**.

Figure 5 The relationship between n-octane and the untreated surface in the hexagonal arrangement (250 µm spacing). The droplet failed to retain form on top of the feature and immediately penetrated into the grooves.

For the FTS treated surfaces, the average angle was much smaller when compared to the DI water. These solutions aligned much more closely with the Wenzel estimated angle as well, showing they would be entering in the wetting state. This makes sense due to their chemical properties and their inability to retain shape on the untreated surface.

Table 5 Shows the FTS surface angles for octane and decane. The feature arrangement, diameter (D), height (H), and spacing (S) are all listed accordingly below. The average angle over the entire tested period (30 minutes) was calculated and shown along with the standard deviation. In addition, the predicted angles from **Equations 1 and 2** for the Wenzel and Cassie-Baxter estimations are shown above.

Surface	**FTS**							
Feature	**250 Spacing**							
Solution	**D (µm)**	**H (µm)**	**S (µm)**	**Average Angle (º)**	**St.dev (º)**	**Average R (µm)**	**Wenzel Estimation (º)**	**C-B Estimation (º)**
Octane	250	1000	250	82	4.3	1.79	75.51	137.86
Decane	250	1000	250	86	2.3	1.74	83.62	139.35

Another surface treatment was considered, OTS, however the retention time for the droplet was too quick for proper analysis. Two videos are included in **Appendix B** to show how the droplet sets on an untreated and FTS treated surface.

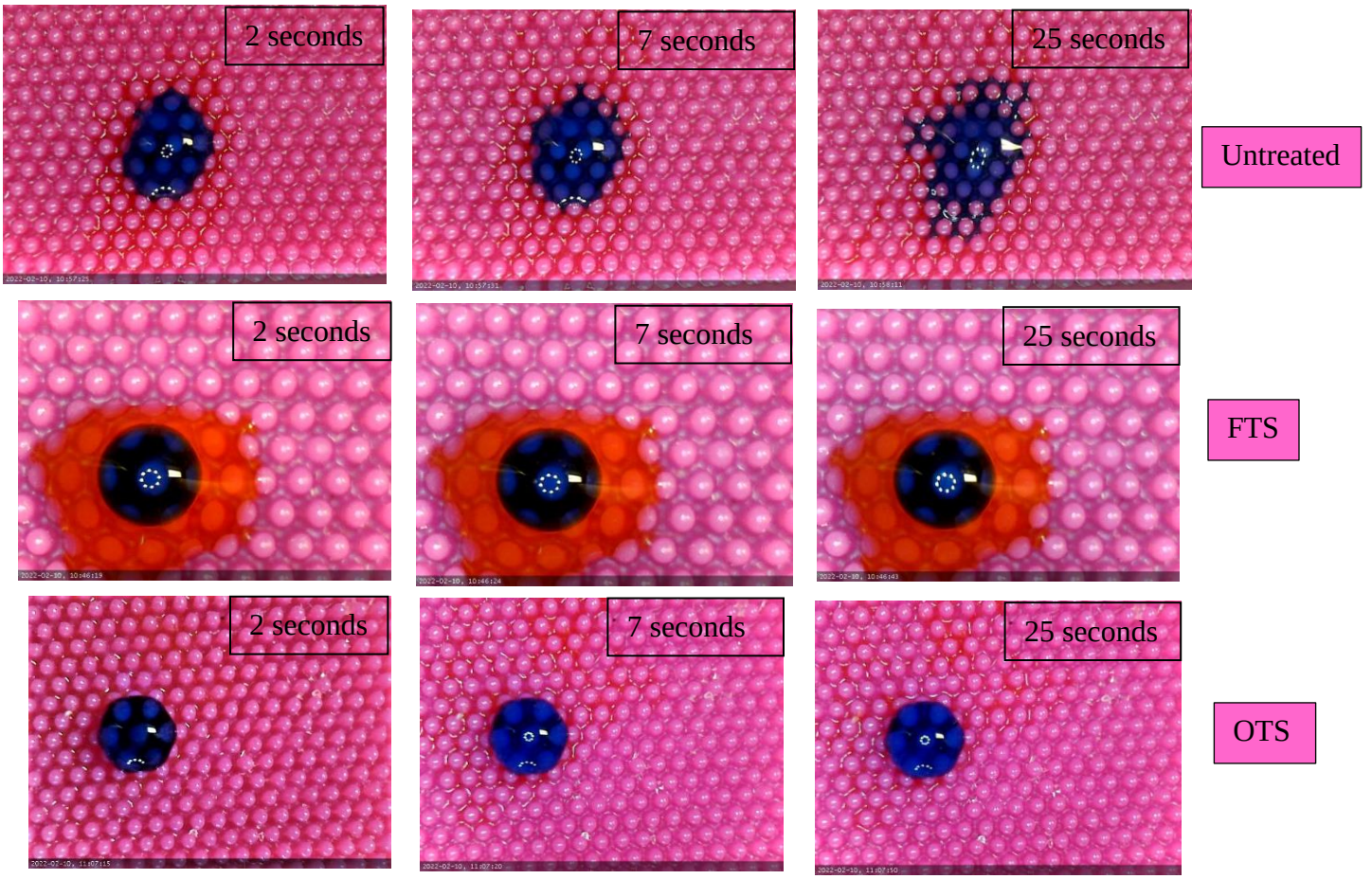

Figure 6 Show the untreated, FTS, and OTS surface with a DI water (blue) and oil (red) mixture at 2, 7, and 25 seconds respectively. As time increases for the general trend, the oil penetrates the grooves and separates from the water. A stronger treated surface showed a stronger separation potential. From these results, an OTS treatment would be the most optimal surface to do a water-oil separation.

Table 6 Shows the calculated evaporation rate for each of the solutions for a 10 µm sized drop. The drop size and loss after 30 minutes are also estimated and calculated below.

Solution	Evaporation (drop/min)	Size (Drop)	Drop Loss
DI Water	0.000134	5.97	4.03
Octane	0.000258	2.25	7.75
Decane	0.000444	0.00	10.00

Discussion and Analysis

The original prediction for the apparent contact angles for DI water was to remain in the Cassie-Baxter state. However, when tested, it was determined the Cassie-Baxter approximation only applied for the FTS treated surface. The untreated surface, instead, correlated more with the Wenzel approximation, which matches past research. However, when enough time passes, the grooves will be penetrated regardless of the treatment.

For the various models involving DI water, it was determined for the spacing the best surface would be in a square configuration with the shortest spacing (250 μm) as possible when treated with FTS. This produced a contact angle of 117±10.9º. For the other square model tested, the second largest angle was 117±1.6º from the untreated surface. Due to these angles being close, the square arrangement has hardly any effect on the initial contact angle. It also held the prediction to stay in the Cassie-Baxter state from the relationship in **Equation 4** for both the untreated and FTS treated surface. For the hexagonal untreated models, the 250 μm spacing had a larger contact angle than the 500 μm spacing with 138±13ºbeing larger than 94±4.1º respectively. The 250 μm remained in the Cassie-Baxter state while the 500 spacing wetted into the Wenzel state. This proves that the smaller the spacing, the more hydrophobic the surface will become. For the FTS treated models, the same relationship held true with the 250 μm angle at >150±0.0º being larger than the 500 μm angle at 114±7.4º. The Cassie-Baxter relationship has limitations for being unable to predict angles above 150º, thus it was impossible to get the exact reading for the 250 μm model.

For the n-octane and n-decane solutions, these produced an angle of 82±4.3º and 86±2.3º respectively. These two stayed in the Wenzel state, as predicted.The longer the carbon chains are, the stronger the initial contact angle became. However, in contrast, the n-decane wetted the surface much quicker than n-octane. For the most hydrophobic result for these types of solutions, it would be wise to use a weaker carbon chain and strongly treated surface.

There are sources of error to consider for this experiment. The measure contact angle from the pipette could have been slightly less than the desired 10 μL. As a result, the droplet radius measurement would overestimate or underestimate the contact angle. The measurements, also, assume the shape of the droplet to be a perfect sphere, which was impossible to ensure with the equipment available. In addition, the humidity of the room was unable to be controlled, thus the droplet could have evaporated faster or slower than anticipated, leading to skewed results. The featured models used also had limitation in their design. The 3D printer utilized had size limitations in addition to limited selection for the shape of the pegs. The pegs were rounded at the top and the printer was unable to produce any other results. For more thorough examination, a flat or concaved top of the pegs would lead to a much more liquid repelling surface.[5]

For future research, steps should be taken to investigate additional geometry dimensions in arrays. More organic liquids should be considered to truly find the relationship between them. Droplet volume can also be a variable to consider when investigating the hydrophobic properties of a surface. This research builds upon previous research conducted. Lee et al. studied the wetting transition on cylindrical pillars made of PDMS for various spacing ratios, much like this report. The increasing spacing ratio led to the contact angle increasing to a peak of a spacing

ratio of 2, and then led to a sharp decreased.[3] This was confirmed to be true as well for this research as smaller contact angles lead to a decreased time to wet the surface. The largely spaced surfaces were past the peak, thus wetted the surface quicker. In addition, Murakami et al. studied cycloolefin polymer surfaces with various ionic liquids to observe their hydrophobic or hydrophilic properties.[4] This report only looked at one plastic resin surface, however, much like Murakami, multiple solutions were analyzed. With this research, an additional perspective is added into the knowledge of this topic and further research can be conducted to better understand how to manipulate the wetting of surfaces.

Literature Cited

[1] Kumar, M., & Bhardwaj, R. *Wetting characteristics of Colocasia esculenta (taro) leaf and a bioinspired surface thereof*. Nature News. Retrieved March 27, 2022, from https://www.nature.com/articles/s41598-020-57410-2

[2] Ananya *How do taro leaves repel water?* Research Matters. Retrieved March 27, 2022, from https://researchmatters.in/news/how-do-taro-leaves-repel-water

[3] Lee, J., Gwon, H., Lee, S., & Cho, M. "Wetting Transition Characteristics on Micro structured Hydrophobic Surfaces." Materials Transactions, vol. 51 no. 9, 2010, pp 1709-1711., doi: 10.2320/matertrans.M2010118.

[4] Murakami, D., et al. "Wetting Transition from the Cassie–Baxter State to the Wenzel State on Textured Polymer Surfaces." Langmuir, vol. 30, no. 8, 2014, pp. 2061–2067. doi:10.1021/la4049067.

[5] Pineault, H. (2021). Wetting Transition of 3D-printed Featured Surface. *Honors Research Project*.

Appendices

Appendix A: Additional Tables

Table A.1 The calculated values for the contact angles (in degrees) using the Wenzel's Estimation **(Equation 1**) of the features for the various treatments.

Wenzel Relationship					
Feature	**θs**	**cosθs**	**r**	**cosθapp**	**θapp**
Untreated Square 1	117.2	-0.457	1.37	-0.6272	128.8
Untreated Square 2	108.4	-0.315	1.44	-0.4528	116.9
Untreated Hexagon (500 µm)	94.6	-0.080	1.56	-0.1257	97.2
Untreated Hexagon (250 µm)	138.1	-0.744	1.27	-0.9474	161.3
FTS Square	117.8	-0.467	1.34	-0.6252	128.7
FTS Hexagon (500 µm)	114.7	-0.418	1.39	-0.5821	125.6
FTS Hexagon (250 µm)	150.0	-0.866	1.01	-0.8720	150.7
FTS Hexagon (250 µm) Decane	86.33	0.064	1.74	0.1112	83.6
FTS Hexagon (250 µm) Octane	81.96	0.140	1.79	0.2503	75.5

Table A.2 The calculated values for the contact angles (in degrees) using the Cassie-Baxter's Estimation (**Equation 2**) of the features for the various treatments.

C-B Relationship		
r	**fs**	**θapp**
1.37	0.196	153.3
1.44	0.196	149.9
1.56	0.101	155.1
1.27	0.227	160.4
1.34	0.196	153.5
1.39	0.101	160.3
1.01	0.227	165.8
1.74	0.227	139.4
1.79	0.227	137.9

Appendix B: Videos

See attached files for the videos.